Electron-phonon coupling in a boron-doped diamond superconductor

H. J. Xiang, Zhenyu Li, Jinlong Yang,* J. G. Hou, and Qingshi Zhu
Hefei National Laboratory for Physical Sciences at Microscale, Laboratory of Bond Selective Chemistry and Structure Research Laboratory, University of Science and Technology of China, Hefei, Anhui 230026, People's Republic of China
(Received 10 July 2004; revised manuscript received 17 September 2004; published 15 December 2004)

The electronic structure, lattice dynamics, and electron-phonon coupling of the boron-doped diamond are investigated using the density-functional supercell method. Our results indicate the boron-doped diamond is a phonon mediated superconductor, confirming previous theoretical conclusions deduced from the calculations employing the virtual-crystal approximation. We show that the optical-phonon modes involving B vibrations play an important role in the electron-phonon coupling. Different from previous theoretical results, our calculated electron-phonon coupling constant is 0.39 and the estimated superconducting transition temperature T_c is 4.4 K for the boron-doped diamond with 2.78% boron content using the Coulomb pseudopotential $\mu^*=0.10$, in excellent agreement with the experimental result.

DOI: 10.1103/PhysRevB.70.212504 PACS number(s): 74.25.Kc, 74.25.Jb, 74.70.Ad, 74.62.Dh

Recently, Ekimov *et al.*[1] reported the discovery of superconductivity in the boron-doped diamond synthesized at high pressure and high temperature. Their measurements showed that the boron-doped diamond with a hole carrier density of 5×10^{21} cm^{-3} is a bulk, type-II superconductor below the superconducting transition temperature $T_c\approx4$ K. Using a simplified McMillan formula[2] by setting the Coulomb pseudopotential μ^* to zero, they estimated the electron-phonon coupling (EPC) constant $\lambda=0.2$, indicative of weak EPC.

Before that, superconductivity in some doped semiconductors had been discovered experimentally,[3,4] and superconductivity in many-valley degenerate semiconductors has been also predicted theoretically.[5] As the first group-IV diamond-type semiconductor with superconducting properties, the boron-doped diamond superconductor has been studied by several groups. Baskaran *et al.*[6] suggested that when the boron doping concentration increases to a critical value $n_c\approx4\times10^{21}$ cm^{-3}, an Anderson-Mott insulator to resonating valence-band (RVB)[7] superconductivity transition takes place. By first-principles density-functional perturbation calculations[8] employing the virtual-crystal approximation (VCA),[9] Boeri *et al.*[10] substantiated that the recently discovered superconductivity below 4 K in 3% boron-doped diamond is caused by the coupling of a few holes at top of the σ-bonding valence band to the optical zone-center phonons, similar to MgB_2,[11–14] albeit in three dimensions. Another first-principles study employing the VCA and frozen phonon method also indicated that the EPC is the likely superconducting mechanism.[15] Regardless of their similar conclusion in these two studies, we note that there are some discrepancies in these two studies, especially in the EPC strength and T_c: $\lambda=0.27$ and $T_c=0.2$ K when $\mu^*=0.10$ for 3% doping concentration in the first study, however, $\lambda=0.55$ and $T_c=9$ K when $\mu^*=0.15$ for 2.5% doping concentration in the second study. The difference in doping concentration makes the discrepancy even more prominent, since larger doping concentration leads to larger λ and T_c. Moreover, although a qualitative agreement with experiment is found in these two studies, some obvious disagreements still exist, in particular, T_c in the first study is too small, and T_c in the second study is too large, although one can obtain $T_c=4$ K by setting μ^* to a somewhat large value, i.e., 0.20. The disagreements between experiment and theory might indicate the inapplicability of the VCA to the newly found boron-doped diamond superconductor. In fact, there are some cases where the VCA failed, e.g., the VCA was inappropriate for calculating the band gaps of GaPN and GaAsN,[16] and it described badly the structural and electronic properties of the quaternary alloy GaAlAsN.[17] On the other hand, although computational demanding, the supercell method is usually reliable.[16,17] To bridge the gap between experiment and theory, and to verify the phonon mediated superconducting mechanism in the boron-doped diamond, here we report a first-principles supercell calculation on the EPC of the boron-doped diamond. Our results support the conventional phonon mediated superconducting mechanism in boron-doped diamond and the calculated T_c is in excellent agreement with the experimental value.

Electronic structure calculations and geometrical optimizations are performed using density-functional theory (DFT)[18,19] in the local-density approximation (LDA).[20,21] The electron-ion interaction is described by ultrasoft pseudopotentials,[22] which allow a low cut-off energy (25 Ry in this work) in the plane-wave expansion. The phonon and EPC calculations are carried out using density-functional perturbation theory in the linear response.[8] Within the phonon mediated theory of superconductivity, T_c can be estimated using McMillan's solution of the Eliashberg equation,[2]

$$T_c=\frac{\omega_{\ln}^{ph}}{1.20}\exp\left\{-\frac{1.04(1+\lambda)}{\lambda-\mu^*(1+0.62\lambda)}\right\}, \qquad (1)$$

where λ is the EPC constant, $\omega_{\ln}^{ph}$ is the logarithmically averaged characteristic phonon frequency, and μ^* is the Coulomb pseudopotential which describes the effective electron-electron repulsion. The EPC constant λ is calculated as an average over the N **q**-points mesh and over all the phonon modes, $\lambda=\Sigma_{\mathbf{q}\nu}\lambda_{\mathbf{q}\nu}/N$, where $\lambda_{\mathbf{q}\nu}$ is the electron-phonon interaction for a phonon mode ν with momentum **q**. The

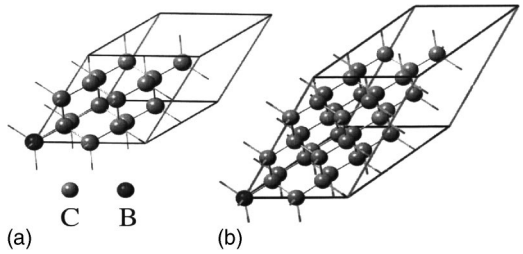

FIG. 1. (Color online) Structures of (a) model I and (b) model II. Refer to the text for the description for the models.

modes responsible for superconductivity can be identified from the Eliashberg function,

$$\alpha^2F(\omega) = \frac{1}{2N}\sum_{\mathbf{q}\nu} \lambda_{\mathbf{q}\nu}\omega_{\mathbf{q}\nu}\delta(\omega - \omega_{\mathbf{q}\nu}). \quad (2)$$

Then $\omega_{\ln}^{ph}$ is calculated as

$$\omega_{\ln}^{ph} = \exp\left\{\frac{2}{\lambda}\int_0^\infty d\omega\alpha^2F(\omega)\ln\,\omega/\omega\right\}. \quad (3)$$

We use the supercell technique to model the boron-doped diamond. In order to study the dependence of the EPC on the doping concentration, we choose two models: $2\times2\times2$ and $3\times3\times2$ diamond supercells with a carbon atom substituted by a boron atom, named models I and II, respectively. The total B content (C_B) for experimental samples is $2.8\pm0.5\%$, which is smaller than the total B content (6.25%) in model I and very close to the total B content (2.78%) in model II. The two models are shown in Fig. 1. The optimized lattice constant for diamond is 3.57 Å, agreeing well with the experimental lattice constant (3.566 Å)[1] and previous theoretical results.[23] For the boron-doped diamond we check that our calculations reproduce the slight lattice expansion, less than 0.3%.[1] Since the not very large boron doping has a negligible effect on the lattice constant of diamond, we use our optimized lattice constant (3.57 Å) in all subsequent calculations.

The *k*-point integration for geometrical optimization, construction of the induced charge density, and calculation of the dynamical matrix is performed over a $4\times4\times4$ ($2\times2\times3$) Monkhorst-Pack grid[24] for model I (II), and a finer $8\times8\times8$ ($4\times4\times6$) grid is used in the phonon linewidth calculations, where the convergence in the *k*-point sampling is more difficult than that for the phonon calculations. The dynamical matrix and phonon linewidth are computed on a $3\times3\times3$ ($2\times2\times3$) **q**-point mesh for model I (II), and a Fourier interpolation is used to obtain complete phonon dispersions.

The Löwdin population analysis has been carried out to get the local density of states (LDOS). The total electronic density of states (TDOS) and LDOS for models I and II are plotted in Fig. 2 (the TDOS for the undoped diamond is also shown as a reference). The TDOS clearly indicates a degenerate or metallic behavior in both models, contrasting sharply with the semiconductor behavior of the undoped diamond. The TDOS and LDOS for model I are very similar with

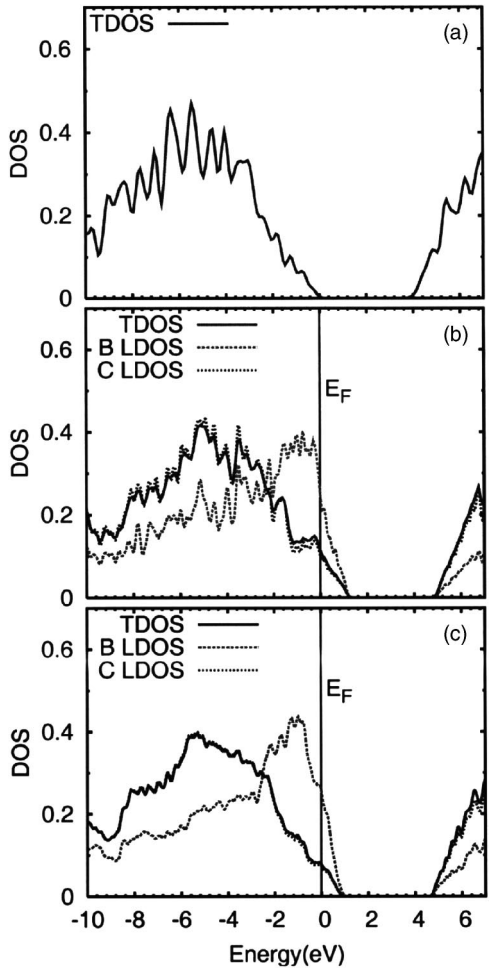

FIG. 2. (Color online) Electronic DOS for the undoped diamond and two boron-doped diamond models. (a) The TDOS of the undoped diamond. (b) and (c) The TDOS and LDOS plots for models I and II. The LDOS for C shown here represents the average LDOS of all the C atoms. TDOS is in states/(spin$\times$eV$\times$diamond unit cell). The unit of LDOS is states/(eV$\times$supercell). Energy is relative to the Fermi level E_F (for the undoped diamond, the valence top is taken as zero-enegy point).

those for model II, except that the width of the acceptor bands (the bands between the valence top and the Fermi level) for model I is larger than that for model II. For both cases, the width of the acceptor bands is larger than that for a boron-doped diamond 64-atom supercell,[25] suggesting a dependence of the width of the acceptor bands on the boron doping concentration. When the doping concentration decreases, the width of the acceptor bands decreases. At very small doping concentration, the acceptor bands even no longer overlap with the valence-band edge of the diamond resulting in a threefold-degenerate acceptor state with a hole binding energy of $E_B \approx 0.37$ eV.[26] Since there are only *s* and *p* electrons in boron-doped diamond, the electron correlation should not be very strong. The metallization in the boron-doped diamond is reasonably caused by the increased boron content, and does not necessarily resort to the Anderson impurity model,[27,28] which is suited for describing strong correlated systems. Figures 2(b) and 2(c) contain the LDOS

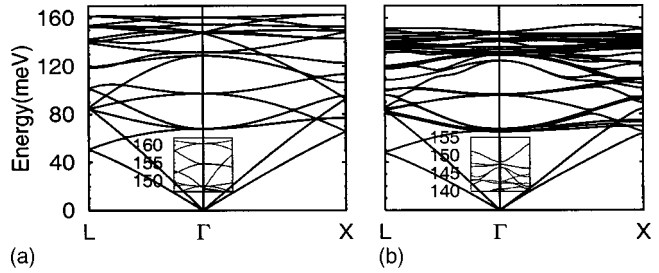

FIG. 3. (Color online) Phonon band structures for (a) $2\times2\times2$ supercell diamond and (b) $2\times2\times2$ supercell diamond with a carbon atom substituted by a boron atom (model I). The insets show the high-energy optical-phonon branches near Γ both for the undoped and doped systems.

plots of the B atom and the average LDOS of the C atoms. From Fig. 2 we can clearly see that the LDOS around the Fermi level for B is larger than that the average LDOS for the C atoms. However, it does not mean the electronic states near the Fermi level are localized around B, since the sum of the LDOS for all C atoms is larger than the LDOS for B.

The calculated frequency of the highest optical phonon at Γ for the undoped diamond is 1295 cm^{-1}, agreeing well with previous LDA calculations,[10,23] and a little smaller than experimental frequency, 1332 cm^{-1}.[1] The phonon band structures for the undoped and boron-doped $2\times2\times2$ diamond supercell are shown in Figs. 3(a) and 3(b), respectively. Here, we plot the phonon band structure for the diamond supercell just for comparison with that for the boron-doped diamond. The phonon band structure for the diamond supercell is more complex than that for the unit cell, since there are much more carbon atoms in the supercell. There are more branches for the boron-doped diamond since some phonon degenerates are removed due to the symmetry breaking, especially since the highest optical phonon at Γ is a onefold A_1 mode, as shown in the inset of Fig. 3(b). Besides that, a general effect to the phonon band structures resulting from the boron doping is the phonon softening; especially, the softening of the optical phonons is sizeable, e.g., the highest frequency of the zone-center optical phonons decreases 99 cm^{-1} to 1196 cm^{-1} for model I. Comparing our results with those obtained from the VCA, we find that the softening of the highest optical-phonon modes at Γ in our supercell calculations is much smaller (the decrease in theirs is 265 cm^{-1} for diamond with 5% boron content[10]). Zhang *et al.* observed that the zone-center optical-phonon line at 1332 cm^{-1} downshifted for boron-doped diamond film.[29] Part of the reason for the downshifting might be the softening of the optical phonon due to the EPC. We can see that there is a slight upturn of the uppermost mode especially when moving from Γ to *X* for both undoped and doped diamond, similar with the previous results.[23,30] Moreover, the upturn for the boron-doped diamond is more noticeable due to the larger EPC for the zone-center optical phonons.

The partial phonon density of states (DOS) for atom *a* is defined as: $\rho_a(\omega)=\Sigma_{\mathbf{q}}\Sigma_{j=1}^{3N}|e_a(\mathbf{q},j)|^2\delta[\omega-\omega(\mathbf{q},j)]$, where *N* is the total number of atoms, $\mathbf{q}$ is the phonon momentum, *j* labels the phonon branch, $e_a(\mathbf{q},j)$ is the phonon displacement vector for atom *a*, and $\omega(\mathbf{q},j)$ is the phonon frequency. The total phonon DOS, B partial phonon DOS, and average partial phonon DOS of all C atoms for both models, are shown in the upper panels of Fig. 4. The shapes of the phonon DOS for these two models are very similar, while the phonon softening effect in model I is stronger due to the larger boron concentration. The lower panels of Fig. 4 are the Eliashberg function $\alpha^2F(\omega)$ for both models. The extremely weak signal in the low-frequency part (lower than 80 meV) of $\alpha^2F(\omega)$ indicates very weak electron acoustic-phonon coupling. Detailed analysis shows that the B-vibrations-related EPC is the largest among all atoms in both models I and II (14.5% in model I and 9.3% in model II). Thus the B-related phonon modes play an important role in the EPC due to the large B electronic LDOS near the Fermi level. As shown in the lower panels of Fig. 4, $\alpha^2F(\omega)$ has sizeable contributions from phonons with medium frequency in our results. However, Boeri *et al.* suggested that $\alpha^2F(\omega)$ vanishes for phonon frequencies below that of the optical zone-center modes, then jumps to a maximum, and finally falls.[10] Their relative simple picture for $\alpha^2F(\omega)$ should stem from the fact that there are only three optical-phonon modes in their virtual-crystal calculations. Since we involve many more phonon modes to calculate $\alpha^2F(\omega)$, our results should be more reliable.

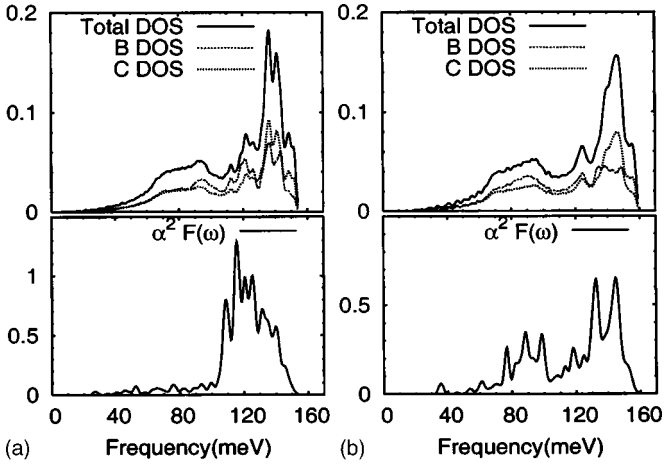

FIG. 4. (Color online) Total phonon DOS, boron partial phonon DOS, and average partial phonon DOS for all carbon atoms, and Eliashberg function $\alpha^2F(\omega)$ for (a) model I and (b) model II. The unit for the total phonon DOS is states/(meV×diamond unit cell). Partial phonon DOS shown here is in arbitrary units.

The calculated TDOS at the Fermi level $[N(E_F)]$, average frequencies $\omega_{\ln}^{ph}$, EPC constants λ, and superconducting transition temperatures T_c for models I and II, are listed in Table I. As expected, the $N(E_F)$ for model I is larger than that for model II due to the larger boron concentration. The $N(E_F)$ for the boron-doped diamond is consistent with the virtual crystal calculations: $N(E_F)$ (in states/(spin×eV ×diamond unit cell) is 0.062 for 2.78% boron versus 0.060 for 2.5% boron,[15] 0.106 for 6.25% boron versus 0.08 for 5% boron.[10] The smaller $N(E_F)$ for the boron-doped diamond than MgB_2 would result in weaker EPC in the boron-doped

TABLE I. Computed electronic DOS at the Fermi level [$N(E_F)$], average frequencies $\omega_{\ln}^{ph}$, EPC constants λ, and superconducting transition temperatures T_c for models I and II. The two values for T_c correspond to two different values of μ^* (0.10 and 0.15). $N(E_F)$ is in states/(spin × eV × diamond unit cell). Boron content C_B is also shown for each model.

	C_B	$N(E_F)$	$\omega_{\ln}^{ph}$ (K)	λ	T_c (K)
Model I	6.25%	0.106	1287	0.56	23.6,11.5
Model II	2.78%	0.062	1218	0.39	4.4,0.9

diamond. The large $\omega_{\ln}^{ph}$ for the boron-doped diamond leads to high T_c, as demonstrated in McMillan's formula.[2] Although the phonon softening increases with increased boron concentration, $\omega_{\ln}^{ph}$ for model I is larger than that for model II, i.e., 1287 K versus 1218 K. The smaller $\omega_{\ln}^{ph}$ for model II results from the substantial EPC in the medium frequency region. The EPC constant λ for model I is 0.56, larger than that ($\lambda=0.39$) for model II. The typical value for μ^* is in the range 0.10–0.15. The calculated T_c for model I is 23.6(11.5) K for $\mu^*=0.10(0.15)$, and for model II it is 4.4(0.9) K for $\mu^*=0.10(0.15)$. The boron concentration for model II is very close to the experimental value and the calculated T_c agrees well with experimental T_c, about 4 K. We can see that T_c increases with increased boron concentration due to the increased λ. A detailed analysis reveals that the EPC is peaked at Γ, which is also found in a previous study.[10] Lee *et al.*[15] overestimated λ and T_c since λ should be averaged over the whole Brillouin Zone (BZ), but their frozen phonon calculations only took into account the zone-center phonons.

Our treatment neglects the anharmonic corrections. For MgB_2, Choi *et al.*[13] showed that λ is decreased from 1.0 to 0.78 after including partial anharmonic corrections. However, more recently, Lazzeri *et al.*[14] suggested that the effects of anharmonicity on T_c and λ in MgB_2 are indeed negligible by explicitly taking into account the scattering between different phonon modes at different **q** points in the whole BZ. Boeri *et al.*[10] considered the anharmonic corrections in the boron-doped diamond using frozen phonon calculations, and found that the effect of anharmonicity is small, i.e., in general λ decreases 0.03 after taking into account the anharmonicity. So, our main results remain essentially unchanged even after including the anharmonic corrections, since the anharmonic corrections for the boron-doped diamond are small, as discussed by Lee *et al.*[15]

In summary, we have carried out a first-principles study on the heavily boron-doped diamond. Optical phonons in diamond are softened after doping with boron. The boron-related vibrational modes contribute an important part to the Eliashberg function $\alpha^2F(\omega)$. Superconductivity in the boron-doped diamond is found to be mediated by the EPC. By using the supercell technique, we resolve the discrepancy between theoretical results based on the VCA and experimental data, and the calculated T_c is in excellent agreement with the experimental result.

This work is partially supported by the National Project for the Development of Key Fundamental Sciences in China (G1999075305, G2001CB3095), the National Natural Science Foundation of China (50121202, 20025309, 10074058), and the USTC-HP HPC project.

*Corresponding author. Email address: jlyang@ustc.edu.cn

[1] E. A. Ekimov, V. A. Sidorov, E. D. Bauer, N. N. Mel'nik, N. J. Curro, J. D. Thompson, and S. M. Stishov, Nature (London) **428**, 542 (2004).
[2] W. L. McMillan, Phys. Rev. **167**, 331 (1968).
[3] J. F. Schooley, W. R. Hosler, and M. L. Cohen, Phys. Rev. Lett. **12**, 474 (1964).
[4] R. A. Hein and E. M. Swiggard, Phys. Rev. Lett. **24**, 53 (1970).
[5] M. L. Cohen, Phys. Rev. **134**, A511 (1964).
[6] G. Baskaran, cond-mat/0404286 (unpublished).
[7] P. W. Anderson, Science **235**, 1196 (1987).
[8] S. Baroni, S. de Gironcoli, A. Dal Corso, and P. Giannozzi, Rev. Mod. Phys. **73**, 515 (2001); S. Baroni, A. Dal Corso, S. de Gironcoli, and P. Giannozzi, http://www.pwscf.org.
[9] L. Nordheim, Ann. Phys. (Leipzig) **9**, 607 (1931).
[10] L. Boeri, J. Kortus, and O. K. Andersen, cond-mat/0404447 (unpublished).
[11] J. Nagamatsu, N. Nakagawa, T. Muranaka, Y. Zenitani, and J. Akimitsu, Nature (London) **410**, 63 (2001).
[12] J. M. An and W. E. Pickett, Phys. Rev. Lett. **86**, 4366 (2001).
[13] H. J. Choi, D. Roundy, H. Sun, M. L. Cohen, and S. G. Louie, Nature (London) **418**, 758 (2002); Phys. Rev. B **66**, 020513(R) (2002).
[14] M. Lazzeri, M. Calandra, and F. Mauri, Phys. Rev. B **68**, 220509(R) (2003).
[15] K.-W. Lee and W. E. Pickett, cond-mat/0404547 (unpublished).
[16] L. Bellaiche, S.-H. Wei, and A. Zunger, Appl. Phys. Lett. **70**, 3558 (1997).
[17] C. Chen, E. G. Wang, Y. M. Gu, D. M. Bylander, and L. Kleinman, Phys. Rev. B **57**, 3753 (1998).
[18] P. Hohenberg and W. Kohn, Phys. Rev. **136**, B864 (1964).
[19] W. Kohn and L. J. Sham, Phys. Rev. **140**, A1133 (1965).
[20] D. M. Ceperley and B. J. Alder, Phys. Rev. Lett. **45**, 566 (1980).
[21] J. P. Perdew and A. Zunger, Phys. Rev. B **23**, 5048 (1981).
[22] D. Vanderbilt, Phys. Rev. B **41**, 7892 (1990).
[23] N. Vast and S. Baroni, Phys. Rev. B **61**, 9387 (2000).
[24] H. J. Monkhorst and J. D. Pack, Phys. Rev. B **13**, 5188 (1976).
[25] A. S. Barnardy, S. P. Russoz, and I. K. Snook, Philos. Mag. **83**, 1163 (2003).
[26] F. Fontaine, J. Appl. Phys. **85**, 1409 (1999).
[27] P. W. Anderson, Phys. Rev. **124**, 41 (1961).
[28] Yu. G. Pogorelov and V. M. Loktev, cond-mat/0405040 (unpublished).
[29] R. J. Zhang, S. T. Lee, and Y. W. Lam, Diamond Relat. Mater. **5**, 1288 (1996).
[30] M. Schwoerer-Böhning, A. T. Macrander, and D. A. Arms, Phys. Rev. Lett. **80**, 5572 (1998).